Available online at www.sciencedirect.com
ScienceDirect
Trans. Nonferrous Met. Soc. China 32(2022) 3088−3098
Transactions of Nonferrous Metals Society of China
www.tnmsc.cn

Electrochemical reduction mechanism of Zn^{2+} in molten NaCl−KCl eutectic

Xiao-bin WU[1], Zeng-li ZHU[1], Hui KONG[1,2], You-qi FAN[1], Si-wei CHENG[1], Zhong-sheng HUA[1,2]

1. School of Metallurgical Engineering, Anhui University of Technology, Ma'anshan 243032, China;
2. Anhui Provincial Key Laboratory of Metallurgical Engineering & Resources Recycling, Anhui University of Technology, Ma'anshan 243002, China

Received 4 August 2021; accepted 29 December 2021

Abstract: A process comprising selective chlorination and molten salt electrolysis was proposed to develop an efficient and environmental-friendly technology for zinc recovery from metallurgical dusts. The theoretical feasibility of this technology was firstly estimated based on thermodynamic fundamentals. Subsequently, the electrochemical behavior of Zn^{2+} on tungsten electrode was investigated in molten NaCl−KCl eutectic at 973 K by many electrochemical transient methods. The results showed that the reduction of Zn^{2+} on tungsten electrode was found to be a one-step process exchanging two electrons with the initial reduction potential of −0.74 V (vs Ag/AgCl), and the electrode process was considered as quasi-reversible and controlled by diffusion. The diffusion coefficient of Zn^{2+} ions in the melts was determined in the order of 10^{-5} cm^2/s. Finally, the electrolytic preparation of zinc was carried out by potentiostatic electrolysis in molten NaCl−KCl−$ZnCl_2$ eutectic at −1.6 V (vs Ag/AgCl). Spheroidic granular metal with silver-white luster was attained after electrolysis for 9.5 h, and identified as pure Zn. The present study confirms that it is practically feasible to extract pure zinc metal by direct electrolysis of $ZnCl_2$ in molten NaCl−KCl eutectic, and provides a valuable theoretical reference for the efficient recovery of zinc from metallurgical dusts.

Key words: electrochemical reduction; zinc ions; electrochemical behavior; molten NaCl−KCl eutectic; metallurgical dusts

1 Introduction

Iron and steel production process is associated with a lot of metallurgical dusts generated in blast furnace, converter and electric arc furnace [1−3]. Although they vary in both physical and chemical compositions, these types of dusts contain not only a large amount of Fe, but also abundant toxic heavy-metal elements such as Zn and Pb to some extent [4,5]. Therefore, the direct discharge of the dusts without any treatment will not only cause serious environmental pollution, but be a waste of valuable metal resources. With the development of metallurgical industry and growing concerns for environmental protection, the treatment and recovery of metallurgical dusts have received increasing attention in current society.

Currently, most of the dusts are often fed directly back into blast furnace or steelmaking process by iron and steel enterprises to recover Fe [6,7]. However, it will lead to the poor operating conditions of the blast furnace and shorten the service life of lining due to the circulation and enrichment of zinc [7−9], and thus it is generally not possible to reutilize all of the dusts in blast furnace application. In this regard, the zinc content in the Fe-bearing dusts should be reduced to a very low level which is permissible in blast furnace application before feeding to a blast furnace for ironmaking. On the other hand, zinc is also a very important base metal required in many industrial

Corresponding author: Hui KONG, Tel: +86-555-2311571, E-mail: konghui@mail.ustc.edu.cn
DOI: 10.1016/S1003-6326(22)66005-9

applications. Thus, a variety of technologies for zinc removal have been developed worldwide to realize the efficient utilization of the Fe-bearing dusts from iron and steel plants. These can be hydrometallurgical, pyrometallurgical, or a combination of both [1,10−14]. Nevertheless, all of the technologies have never reached industrial application because of both economic and technical inefficiencies [4,6]. Therefore, developing a more effective technology for zinc removal is very critical for the recovery of metallurgical dusts.

Chlorination metallurgy is acknowledged as a highly selective and cost-effective technique for the extraction of valuable metals [15−21] due to the thermodynamic difference in formation of various chlorides as well as the low fusion point and high volatility of the generated chlorides [15,22]. It was reported that the Zn-bearing phases such as ZnO and $ZnFe_2O_4$ in steelmaking dusts could be converted to $ZnCl_2$ via chlorination roasting [9]. Subsequently, how to recover zinc from the separated $ZnCl_2$ is another important issue which should be resolved for the harmless disposal and comprehensive utilization of the metallurgical dusts. Molten salt electrolysis is an important and effective approach for metal production due to its short process flow, relatively low energy consumption and pollution [23,24]. Thus, the combined technology based on chlorination and molten salt electrolysis would be a promising approach for zinc recovery from metallurgical dusts. To verify that the proposed recycling route is practically applicable, the electrolytic production of zinc metal through molten salt electrolysis should be investigated. Although the formation of zinc alloys via electrochemical co-reduction with Zn^{2+} or under-potential deposition of reactive metals on liquid Zn cathode has been extensively investigated, reports on electrochemical reduction mechanism of Zn^{2+} in molten NaCl−KCl eutectic are quite limited in current literature [25−29].

Based on the basic thermodynamic evaluation, the electrochemical reduction process of Zn^{2+} on an inert tungsten electrode in eutectic NaCl−KCl melts was fully clarified in the present work. Afterward, the electrolytic production of zinc metal was directly carried out in molten NaCl−KCl−$ZnCl_2$ to demonstrate the feasibility of the proposed route for zinc recovery from the metallurgical dusts.

2 Experimental

The anhydrous NaCl (≥99.5 wt.%), KCl (≥99.5 wt.%) and $ZnCl_2$ (≥99 wt.%) were purchased from Sinopharm Chemical Reagent Co., Ltd. The NaCl−KCl mixture with eutectic composition (molar ratio of 50.6:49.4) was firstly dried at 473 K for more than 72 h to remove the residual moisture, and then fused in a corundum crucible placed in an electric furnace at 973 K. Afterward, the metal ion impurities in the melts were wiped off by pre-electrolysis for 90 min at −2.10 V (vs Ag/AgCl). The anhydrous $ZnCl_2$ was introduced directly into the melts as the source of Zn^{2+} ions. All electrochemical experiments with the melts were operated in a high-purity argon atmosphere to keep off exposure to oxygen and water.

A series of electrochemical measurements including cyclic voltammetry (CV), square wave voltammetry (SWV), chronopotentiometry (CP) and potentiostatic electrolysis, were performed using an electrochemical workstation PARSTAT 2273 (Ametek Group Co., American) controlled by the PowerSuite software package. All electrochemical experiments were carried out in a three-electrode cell, as shown in Fig. 1. A tungsten wire (diameter of 1 mm, 99.99% purity) was polished and thus served as the working electrode, and a spectral pure graphite rod (diameter of 6 mm) was employed as the working electrode. The active surface area of the working electrode was calculated according to its immersion depth in the melts. The reference electrode was a home-made

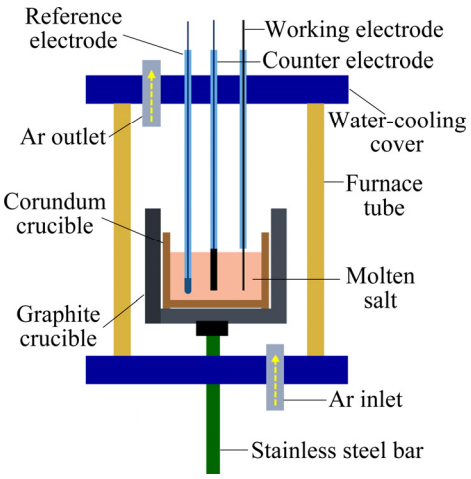

Fig. 1 Schematic diagram of electrochemical experiment set-up

Ag/AgCl electrode, which was a mullite tube containing a silver wire (diameter of 1 mm, 99.99% purity) dipped into NaCl−KCl−AgCl (2 mol.%) melts. All potentials measured in this study were referred to this Ag/AgCl couple.

Zinc metal was extracted from NaCl−KCl−$ZnCl_2$ melts by potentiostatic electrolysis on a tungsten electrode at 973 K. After electrolysis, the obtained metallic products were washed by deionized water to remove the deposited salts and further ultrasonically cleaned in ethanol bath, and then dried in vacuum and stored in a glove box before analysis. The crystal structures of the products were determined by X-ray diffraction (XRD, Bruker D8 Advance) at 40 kV and 40 mA using a Cu K_α radiation. The morphology and element composition of the products were examined by scanning electron microscopy (SEM, JEOL JSM−6490LV) at an accelerating voltage of 15 kV and energy dispersion spectroscopy (EDS) equipped with SEM.

3 Results and discussion

3.1 Process fundamentals and primary thermodynamic evaluation

By considering the potential disadvantages of chlorination metallurgy and molten salt electrolysis mentioned above, a new complete route for recycling zinc from metallurgical dusts is proposed as illustrated in Fig. 2. Fe is the most abundant element in metallurgical dusts. It is expected that the Fe-bearing phases still exist as oxides or metal in solid states after chlorination roasting, and thus can be utilized as a kind of raw material for iron production. Chlorination metallurgy has the distinctive characteristic of high selectivity for metal separation. To predict the feasibility of selective chlorination, the predominant phase diagram of the Fe−Zn−O−Cl system at 973 K was thermodynamically evaluated using FactSage thermochemical software, as indicated in Fig. 3. By controlling the partial pressures of Cl_2 and O_2 in the stable region of $ZnCl_2$(l) (as shown in the blue shadow area), selective chlorination of zinc can be achieved while the Zn-bearing phases will be left in solid Fe_2O_3, Fe_3O_4, FeO and Fe. Although the other species in the dusts such as CaO, Al_2O_3 and PbO may also be chlorinated to the corresponding chlorides especially when residual carbon is contained, pure $ZnCl_2$ can be separated out by taking advantage of the difference in boiling temperature and vapor pressure [15,19,30].

The separated $ZnCl_2$ can be directly introduced into molten chlorides and processed with molten salt electrolysis to yield zinc metal. Molten chloride electrolysis is often conducted in the eutectic melts comprising LiCl, NaCl, KCl, and $CaCl_2$. It can be seen from Fig. 4 that the theoretical decomposition voltage for $ZnCl_2$ is much lower than those for

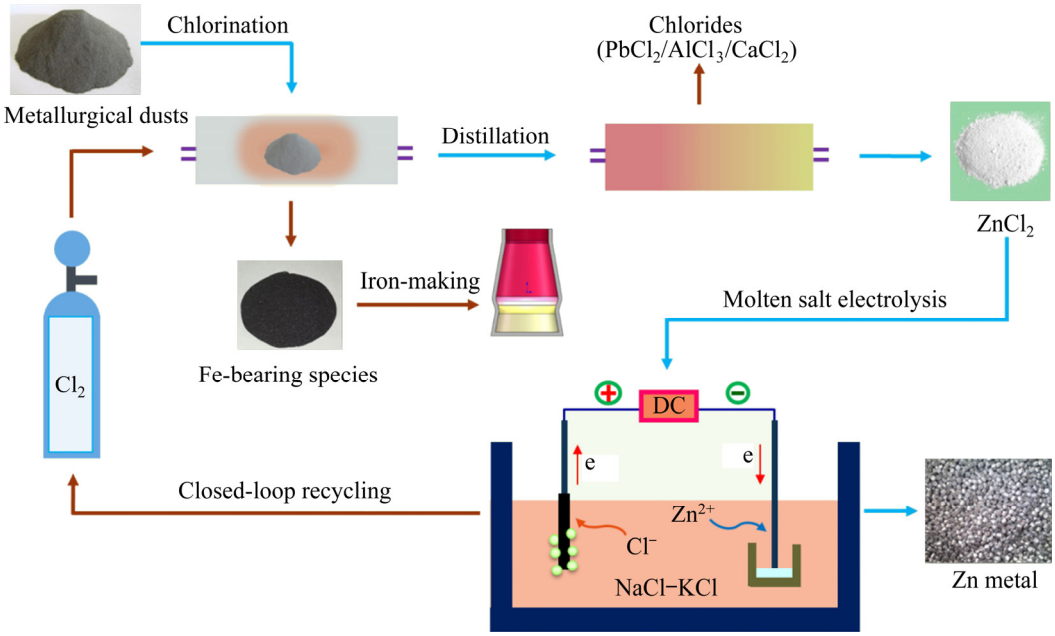

Fig. 2 Flowsheet for zinc recovery from metallurgical dusts

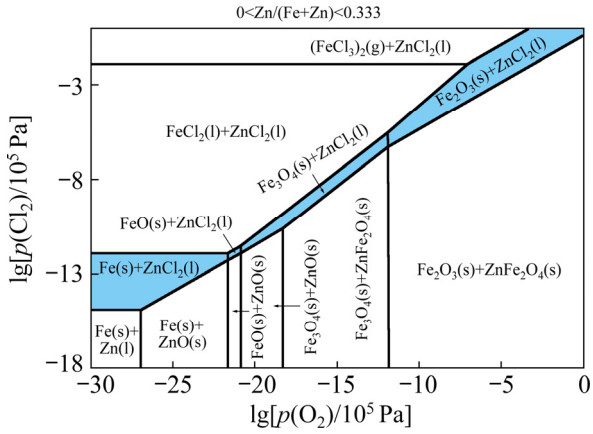

Fig. 3 Predominant phase diagram of Fe−Zn−O−Cl system at 973 K predicted by FactSage software at $0<x(\mathrm{Zn})/x(\mathrm{Fe+Zn})<0.333\%$

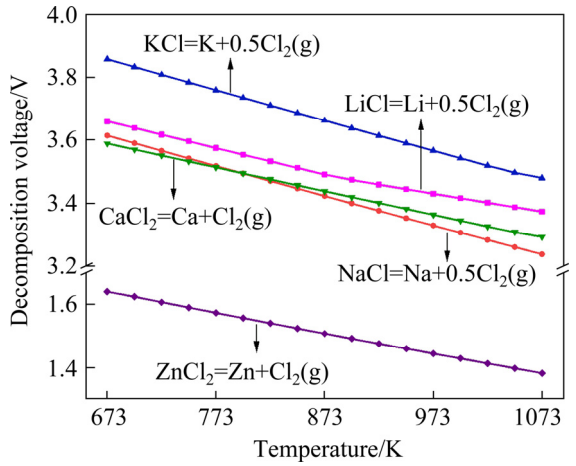

Fig. 4 Theoretical decomposition voltages for various chlorides at different temperatures

other chlorides. This demonstrates that Zn^{2+} ions in the multicomponent melts should be preferentially reduced to Zn metal on the cathode, while the reduction of alkali metal or alkaline-earth metal ions during electrolysis will be less prevalent electrochemically. In the present study, molten NaCl−KCl eutectic was adopted as the supporting electrolyte due to the favorable physicochemical properties and relatively low costs [31,32]. Therefore, the separation of the zinc as chloride from metallurgical dusts and subsequently direct extraction of zinc metal from molten chlorides would be feasible.

This novel process for the recovery of zinc metal from metallurgical dusts shows favorable superiorities from an industrial point of view for the following considerations. Firstly, the whole process is fairly simple due to only two processing steps of chlorination roasting and molten salt electrolysis involved, and pure zinc metal can be recovered. Secondly, the Fe-bearing species still exist in solid oxides or metal phases during selective chlorination, and thus can be comprehensively recovered as raw material for iron-making. Thirdly, the chlorine gas generated in electrolysis can be reused as the chlorinating reagent and no environmentally harmful gases are emitted due to the closed chlorine circulation. Finally, compared with traditional electrowinning of zinc in sulfuric acid solution, molten salt electrolysis is an economically attractive method for zinc extraction because of its high current density and productivity without the limitation stemming from H_2 evolution [20,33].

3.2 Electrochemical behavior of Zn^{2+} in molten NaCl−KCl

The electrochemical behavior of Zn^{2+} was firstly investigated with a tungsten working electrode in molten NaCl−KCl eutectic at 973 K. Figure 5(a) displays CV curves measured in the melts before (red dotted line) and after (blue solid line) adding 1.0 mol.% $ZnCl_2$. The dotted line in Fig. 5(a) shows the representative voltammogram for blank NaCl−KCl eutectic. The sharp negative current spike A_1 at −2.29 V corresponds to the reduction of Na^+ to Na, and the large positive current peak A_2 in the reverse scanning is ascribed to the subsequent dissolution of metallic Na to Na^+. Except for the redox peaks A_1 and A_2, no other redox signals are present in the electrochemical window, confirming that the pure NaCl−KCl eutectic is applicable for the electrochemical investigation. The solid line in Fig. 5(a) presents the CV curve obtained on tungsten electrode with the addition of $ZnCl_2$ to the melts. New redox peaks B_1 and B_2 are observed. As can be seen, the reduction current begins to increase at −0.74 V in the negative-going scan, which is attributed to the reduction of Zn^{2+} to Zn metal. This approximately coincides with the result obtained by theoretical calculation, since the theoretical decomposition voltage of $ZnCl_2$ at 973 K is about 1.8 V lower than that of NaCl, as indicated in Fig. 4. In the positive-going sweeping, the oxidation signal B_2 with a much higher amplitude corresponds to the subsequent re-oxidation of Zn metal. Additionally, the reduction peak B_1 present in the voltammogram is apparent, suggesting that the electrochemical

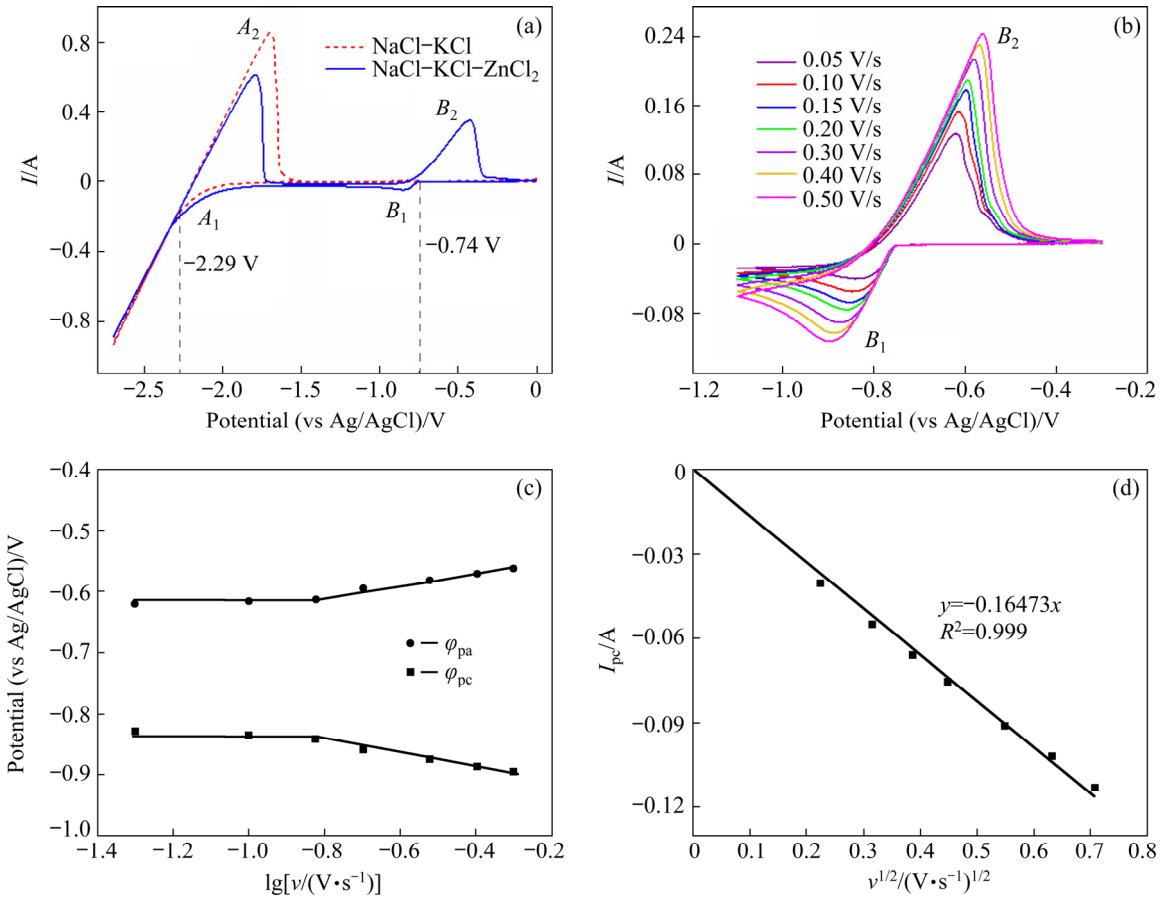

Fig. 5 CV curves attained with tungsten electrode in NaCl−KCl eutectic melts: (a) Before and after addition of 1.0 mol.% $ZnCl_2$ with scan rate of 0.1 V/s; (b) Within scan range from −0.3 to −1.1 V at varied scan rates; (c) Variation of anodic and cathodic peak potentials with logarithm of scan rate; (d) Dependence of cathodic peak current on square root of scan rate (Temperature: 973 K; area S=0.32 cm^2)

reduction of Zn^{2+} to Zn on tungsten electrode in the molten NaCl−KCl is diffusion-limited [34]. Obviously, no other signal couples except for A_1/A_2 and B_1/B_2, exist in the CV curve for NaCl−KCl−$ZnCl_2$ melts, manifesting that zinc metal could be electrodeposited on the tungsten electrode directly via the following reaction:

$$Zn^{2+}+2e=Zn \quad (1)$$

Subsequently, a series of CVs over a wide scan rate range from 0.05 to 0.50 V/s were recorded on tungsten electrode to evaluate the reversibility of the redox reaction of Zn^{2+}/Zn in molten NaCl−KCl, as exhibited in Fig. 5(b). In the case of a completely reversible electrode reaction, the absolute value of the difference between anodic and cathodic peak potentials ($|\varphi_{pa}-\varphi_{pc}|$) should be a constant value of 0.094 V for a two-electron transferred reaction at 973 K. As indicated in Fig. 5(c), both anodic and cathodic peak potentials stay relatively stable and the value of $|\varphi_{pa}-\varphi_{pc}|$ shows no remarkable changes at low scan rates. It is noteworthy that the value of $|\varphi_{pa}-\varphi_{pc}|$ is obviously higher than 0.094 V, which is probably related to the ohmic drop in the electrolytic cell and the experimental operations [35]. Similar phenomena have also been observed in previous studies [29,36]. However, at higher scan rates, the cathodic and anodic peak potentials shift negatively and positively, respectively, and the value of $|\varphi_{pa}-\varphi_{pc}|$ increases as the scan rate increases. Therefore, the redox process of Zn^{2+}/Zn on tungsten electrode in molten NaCl−KCl is considered not to be fully reversible, but quasi-reversible. Meanwhile, the dependence of the cathodic peak current (I_{pc}) on the square root of the potential scan rate ($v^{1/2}$) for the molten NaCl−KCl−$ZnCl_2$ is illustrated in Fig. 5(d). It is clear that I_{pc} depends linearly on $v^{1/2}$, suggesting that the electrochemical reduction of Zn^{2+} to Zn in molten NaCl−KCl eutectic is controlled by the

diffusion rate. For a quasi-reversible soluble/insoluble system, the diffusion coefficient (D) of Zn^{2+} ions in the melts can be quantitatively estimated by the Berzins−Delahay equation according to the theory of CV [37]:

$$I_{pc}=-0.61Sc_0(nF)^{3/2}D^{1/2}v^{1/2}(RT)^{-1/2} \quad (2)$$

where S is the electrode surface area (cm^2), c_0 represents the concentration of electroactive species (mol/cm^3), n is the number of electrons exchanged in the reaction, F corresponds to the Faraday constant (96485 C/mol), R is the mole gas constant (8.314 J/(mol·K)), and T denotes the thermodynamic temperature (K). According to the slope of the fitting line in Fig. 5(d), the diffusion coefficient of Zn^{2+} ions in this system is calculated to be 1.8×10^{-5} cm^2/s by assuming two electrons exchanged in the reaction.

SWV is a sensitive technique which can be used to determine the number of electrons exchanged in the electrochemical reaction. Subsequently, the reduction process of Zn^{2+} in molten NaCl−KCl eutectic was further investigated by SWV. Figure 6(a) shows a series of square wave voltammograms collected on a tungsten electrode in molten NaCl−KCl−$ZnCl_2$ (1 mol.%) at frequencies of 10−50 Hz and a step potential of 2 mV at 973 K. It is evident that the asymmetric Gaussian peak located at around −0.8 V is associated with the reduction of Zn^{2+}, which is consistent with that measured by CV. Moreover, the peak current increases with the increase of frequency. As shown in the inset of Fig. 6(a), the peak current demonstrates basically a linear relationship with the square root of the frequency, further implying that the reduction of Zn^{2+} can be regarded as a quasi-reversible process. It should be pointed out that the asymmetry for peak in Fig. 6(a) is correlated with the overpotential during the electrochemical reduction of Zn^{2+} to the liquid Zn metal. The increase of the current during the reduction process is delayed due to the overpotential, and thus the increasing part of the current for the peak is steeper than the decreasing part. Similar phenomena have also been observed in the electrodeposition of lead and tin metal in molten chlorides [22,38]. Accordingly, only the decreasing part of peak is taken into account for measuring the half-wave width ($W_{1/2}$) of the redox peak. According to this methodology, the $W_{1/2}$ value of peak is obtained to be 0.16 V, as depicted by the Gaussian fitting curve in Fig. 6(b). Thus, the number of exchanged electrons (n) can be estimated by the following equation:

$$W_{1/2}=3.52\frac{RT}{nF} \quad (3)$$

The number of electrons transferred is calculated to be 1.84, which is close to 2, further confirming that the reduction of Zn^{2+} to Zn metal should proceed through a single step with two electrons transferred.

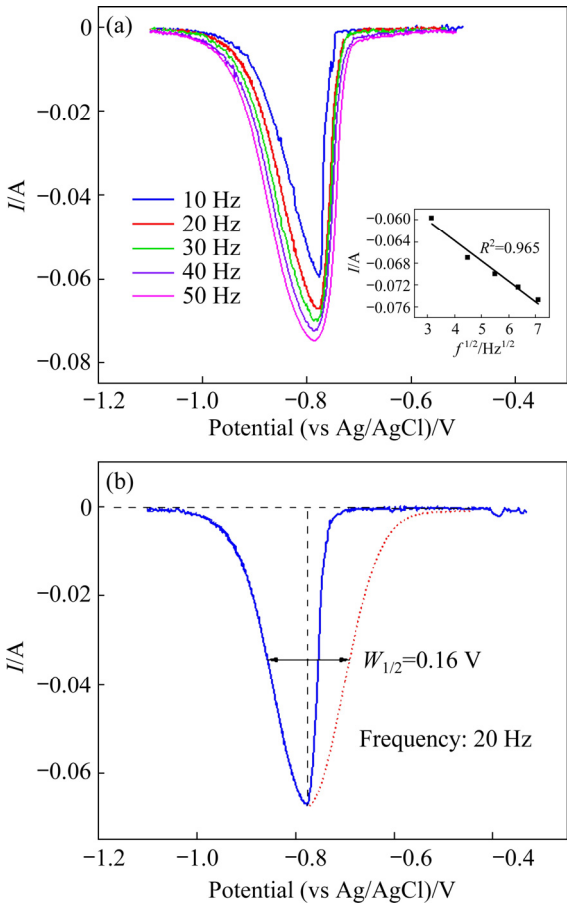

Fig. 6 SWV curves measured on tungsten electrode in molten NaCl−KCl−$ZnCl_2$ (1 mol.%) at various frequencies (a) and 20 Hz (b) with Gaussian fitting (Temperature: 973 K; S=0.32 cm^2; amplitude: 25 mV; potential step: 2 mV)

CP was also carried out to further investigate the electrochemical reduction of Zn^{2+} in the molten NaCl−KCl. Figure 7(a) exemplifies the chronopotentiograms attained on a tungsten electrode in molten NaCl−KCl−$ZnCl_2$ (1 mol.%) at 973 K with the applied current from −80 to −30 mA. Two potential plateaus are present in a series of CP

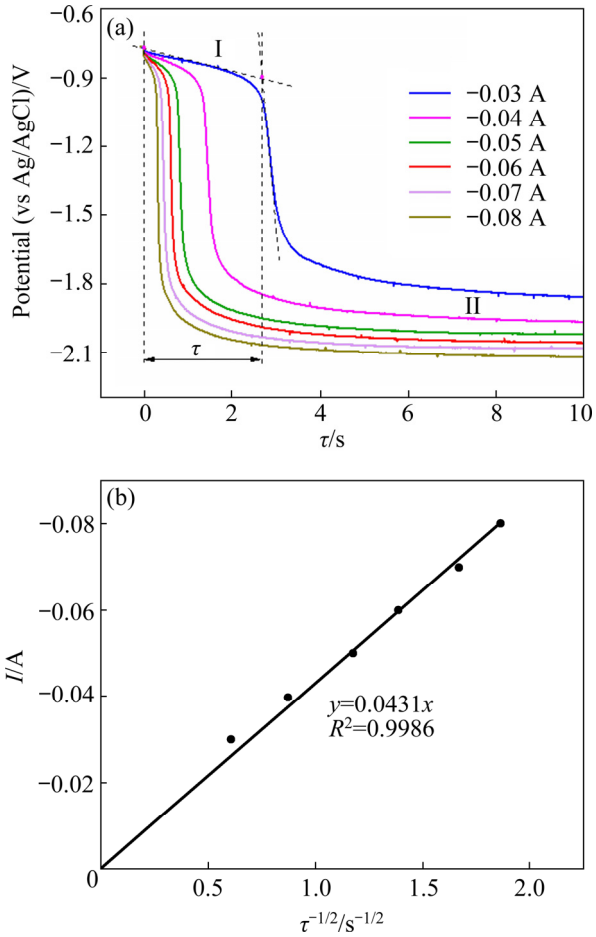

Fig. 7 CP curves obtained on tungsten electrode in molten NaCl−KCl−$ZnCl_2$ (1 mol.%) at 973 K (a) and variation of current with reciprocal square root of transition time $\tau^{-1/2}$ (b) (S=0.32 cm^2)

curves. The potential Plateau I at around −0.8 V corresponds to the deposition of zinc metal. Afterward, the cathodic potential steadily increases to a limited value with increasing the current, and a more negative potential Plateau II appears, which is ascribed to the signal for the reduction of Na^+ ions. The two plateaus are in the same potential ranges as detected in CV and SWV curves. Moreover, it is evident that the negative shift of Plateau I is unconspicuous and independent of the current, further proving that the reduction of Zn^{2+} in the system is a diffusion controlled process. Herein, transition time (τ) represents the necessary time for the complete depletion of Zn^{2+} ions originated from the layer of electrolyte around the electrode surface through diffusion, and decreases as the applied current increases. The transition time for zinc reduction was measured by the method introduced in Ref. [39]. As shown in Fig. 7(b), the square root of the transition time ($\tau^{-1/2}$) varies linearly with respect to current (I). Hence, according to the slope of the fitted line, the diffusion coefficient (D) of Zn^{2+} in the melts can also be determined by the following Sand equation [40]:

$$I\tau^{1/2} = 0.5\pi^{1/2}nFSc_0D^{1/2} \quad (4)$$

The diffusion coefficient of Zn^{2+} in molten NaCl−KCl eutectic at 973 K is calculated to be 1.4×10^{-5} cm^2/s, which is close to that determined by using the Berzins−Delahay equation.

3.3 Extraction and characterization of zinc metal

Based on the above investigations, potentiostatic electrolysis was carried out on a tungsten electrode at −1.6 V, to verify the feasibility of electrochemical extraction of zinc metal from molten chlorides. Figure 8 exhibits the current evolution during electrolysis in molten NaCl−KCl−$ZnCl_2$ (1 mol.%) at 973 K. As the electrolysis proceeds, the surface area of the electrode is slightly enlarged due to the deposition of zinc on the electrode, and thus the current keeps increasing slowly, from −0.10 to −0.17 A in a long period of 2.5×10^4 s. Since the melting point of zinc metal (693 K) is lower than the electrolysis temperature, liquid zinc metal is deposited on the tungsten electrode. Liquid drops of zinc metal fall off occasionally from the electrode caused by the shrinkage of the liquid surface and the changes of surface tension, and consequently the surface area

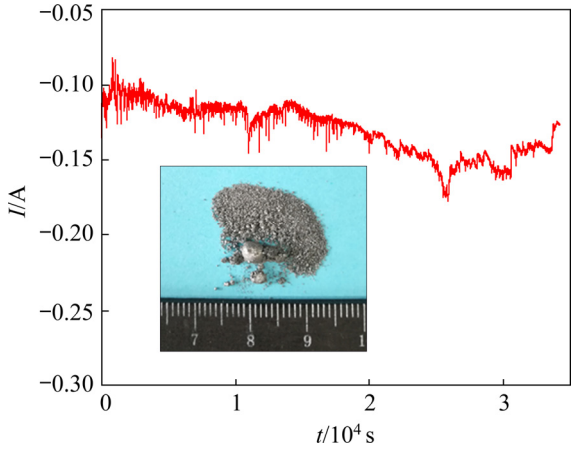

Fig. 8 Typical evolution of current during potentiostatic electrolysis at −1.6 V acquired on tungsten electrode in molten NaCl−KCl−$ZnCl_2$ (1 mol.%) at 973 K (Inset: Zinc granules obtained after potentiostatic electrolysis for 9.5 h)

of the electrode decreases again. Metallic zinc granules of various sizes were collected at the bottom of the melts, as shown in the inset in Fig. 8. After a long-term electrolysis, the current gradually decreases because of the serious depletion of Zn^{2+} ions in the melts. It is noteworthy that the current fluctuates, which can be ascribed to the variation of the electrode surface by the deposition and fall-off of liquid zinc metal.

After the potentiostatic electrolysis on the tungsten electrode at −1.6 V for 9.5 h in molten NaCl− KCl−$ZnCl_2$ (1.0 mol.%) at 973 K, spheroidal metallic granules with silver-white luster have be extracted from the melts. Figure 9 depicts the XRD pattern of the products. The diffraction peaks are identified as pure Zn, and no other phases have been detected. The SEM image (Fig. 10(a)) shows that the obtained zinc metal is compact in microstructure without other impure inclusions. Figures 10(b) and (c) show the EDS results for Points *A* and *B* taken from Fig. 10(a), respectively. The contents of Zn for Points *A* and *B* are 100%, further confirming that the obtained product is pure Zn. Therefore, it is technically feasible to extract zinc metal through direct electrolysis of $ZnCl_2$ in molten NaCl−KCl eutectic.

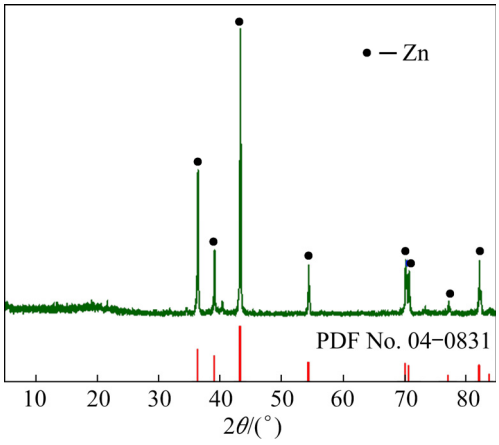

Fig. 9 XRD pattern of products obtained by potentiostatic electrolysis at −1.6 V for 9.5 h in molten NaCl−KCl−$ZnCl_2$ (1 mol.%) at 973 K

4 Conclusions

(1) A processing route based on selective chlorination and molten salt electrolysis was proposed in the present study to efficiently recover zinc from metallurgical dusts. Thermodynamic calculation results manifest that ZnO in metallurgical

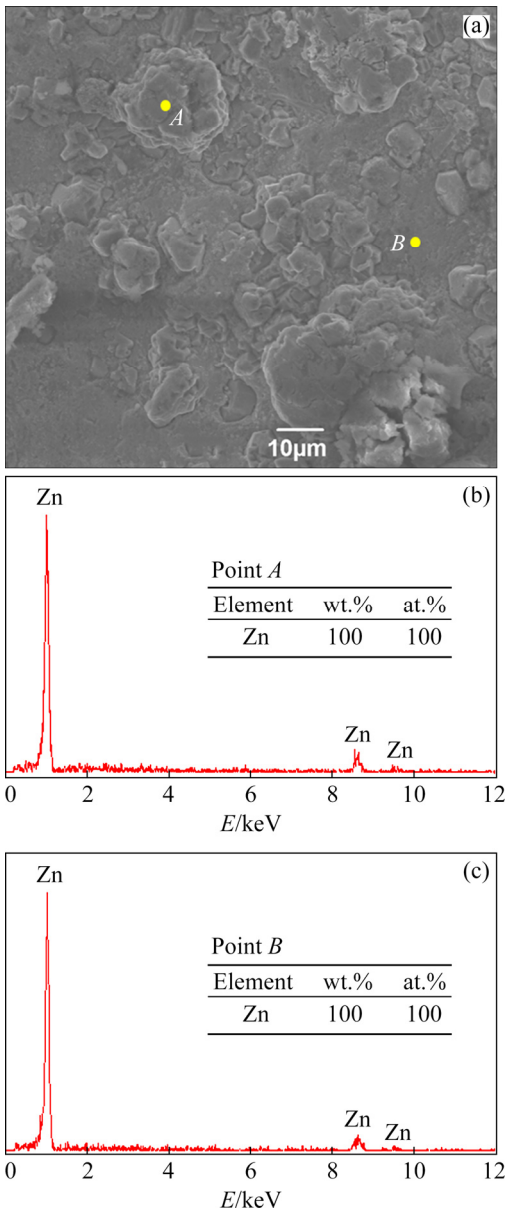

Fig. 10 SEM image (a) and EDS results (b, c) of products obtained by potentiostatic electrolysis at −1.6 V for 9.5 h in molten NaCl−KCl−$ZnCl_2$ (1 mol.%) at 973 K

dusts can be selectively converted to $ZnCl_2$ while the Fe-bearing species will still be left in solid states. The obtained $ZnCl_2$ will be preferentially reduced to Zn metal by electrolysis in molten chlorides because of its comparatively low decomposition voltage. These imply that the proposed route is theoretically feasible and will be an alternative approach for the zinc recovery from metallurgical dusts.

(2) The electrochemical behavior of Zn^{2+} in the molten NaCl−KCl eutectic at 973 K was investigated on a tungsten electrode using CV, SWV and CP. The results indicate that Zn^{2+} is

directly reduced to Zn metal in molten NaCl−KCl eutectic through a single step with two electrons transferred, and the initial reduction potential is −0.74 V. The electrode reaction of Zn^{2+}/Zn couple in molten NaCl−KCl is found to be a quasi-reversible process controlled by the diffusion of Zn^{2+}. The diffusion coefficient of Zn^{2+} in NaCl−KCl eutectic at 973 K was calculated to be approximately 1.8×10^{-5} and 1.4×10^{-5} cm^2/s by using the Berzins−Delahay equation and the Sand equation according to the results of CV and CP, respectively.

(3) Potentiostatic electrolysis was conducted at −1.6 V in molten NaCl−KCl−$ZnCl_2$ (1 mol.%) at 973 K. Spheroidic bulk metal with silver-white luster was obtained after electrolysis for 9.5 h. The electrolytic products were identified to be pure Zn metal by XRD and SEM−EDS analyses. These results confirm that zinc metal can directly be extracted from $ZnCl_2$ by electrolysis in molten NaCl−KCl eutectic, implying that the proposed process is technically applicable for recovery of zinc from metallurgical dusts.

Acknowledgments

The authors are grateful for the financial support from the Natural Science Foundation of Anhui Province, China (No. 2008085ME170), the Anhui Special Support Plan, China (No. T000609), and the National Natural Science Foundation of China (No. 51204002).

References

[1] ZHANG Jin-xia, LIU Shu-xian, NIU Fu-sheng, XU Zhi-shuai. Reviews on the comprehensive utilization of metallurgical dust from iron and steel plant [J]. Applied Mechanics and Materials, 2013, 295/296/297/298: 3075−3079.

[2] DROBÍKOVÁK, PLACHÁD, MOTYKA O, GABOR R, KUTLÁKOVÁK M, VALLOVÁ S, SEIDLEROVÁ J. Recycling of blast furnace sludge by briquetting with starch binder: Waste gas from thermal treatment utilizable as a fuel [J]. Waste Management, 2016, 48: 471−477.

[3] ZHANG Mei, LI Wen-song, WANG Wei-yan, LIU Wen-ying, FU Zhi-gang, YANG Yun-quan. Recovery of potassium chloride from blast furnace flue dust [J]. RSC Advances, 2015, 5(103): 84901−84909.

[4] PENG Cui, ZHANG Fu-li, LI Hui-fang, GUO Zhan-cheng. Removal behavior of Zn, Pb, K and Na from cold bonded briquettes of metallurgical dust in simulated RHF [J]. ISIJ International, 2009, 49(12): 1874−1881.

[5] YEHIA A, EL-RAHIEM F H. Recovery and utilization of iron and carbon values from blast furnace flue dust [J]. Mineral Processing and Extractive Metallurgy, 2005, 114(4): 207−211.

[6] LIU Xing-le, LIU Zheng-lian, ZHANG Jian-liang, XING Xiang-dong. Recovery of iron and zinc from blast furnace dust using iron-bath reduction [J]. High Temperature Materials and Processes, 2019, 38: 767−772.

[7] GAO Zhi-fang, WU Zhao-jin, ZHENG Ming-dong. Effect of blast furnace sludge on SO_2 emissions from coal combustion [J]. Energy & Fuels, 2016, 30(4): 3320−3330.

[8] KUKURUGYA F, VINDT T, HAVLÍK T. Behavior of zinc, iron and calcium from electric arc furnace (EAF) dust in hydrometallurgical processing in sulfuric acid solutions: Thermodynamic and kinetic aspects [J]. Hydrometallurgy, 2015, 154: 20−32.

[9] JAAFAR I, GRIFFITHS A J, HOPKINS A C, STEER J M, GRIFFITHS M H, SAPSFORD D J. An evaluation of chlorination for the removal of zinc from steelmaking dusts [J]. Minerals Engineering, 2011, 24(9): 1028−1030.

[10] DAS B, PRAKASH S, REDDY P S R, MISRA V N. An overview of utilization of slag and sludge from steel industries [J]. Resources, Conservation and Recycling, 2007, 50(1): 40−57.

[11] XIA D K, PICKLESI C A. Microwave caustic leaching of electric arc furnace dust [J]. Minerals Engineering, 2000, 13(1): 79−94.

[12] HAN Jun-wei, LIU Wei, QIN Wen-qing, PENG Bing, YANG Kang, ZHENG Yong-xing. Recovery of zinc and iron from high iron-bearing zinc calcine by selective reduction roasting [J]. Journal of Industrial and Engineering Chemistry, 2015, 22: 272−279.

[13] SINHA M K, PRAMANIK S, SAHU S K, PRASAD L B, JHA M K, PANDEY B D. Development of an efficient process for the recovery of zinc and iron as value added products from the waste chloride solution [J]. Separation and Purification Technology, 2016, 167: 37−44.

[14] LECLERC N, MEUX E, LECUIRE J M. Hydrometallurgical extraction of zinc from zinc ferrites [J]. Hydrometallurgy, 2003, 70(1/2/3): 175−183.

[15] LI Jin-hui, LI Yang-yang, GAO Yan, ZHANG Yun-fang, CHEN Zhi-feng. Chlorination roasting of laterite using salt chloride [J]. International Journal of Mineral Processing, 2016, 148: 23−31.

[16] ZHOU Shi-wei, WEI Yong-gang, LI Bo, WANG Hua, MA Bao-zhong, WANG Cheng-yan. Chloridization and reduction roasting of high-magnesium low-nickel oxide ore followed by magnetic separation to enrich ferronickel concentrate [J]. Metallurgical and Materials Transactions B, 2016, 47(1): 145−153.

[17] LI Hao-yu, MA Ai-yuan, SRINIVASAKANNAN C, ZHANG Li-bo, LI Shi-wei, YIN Shao-hua. Investigation on the recovery of gold and silver from cyanide tailings using chlorination roasting process [J]. Journal of Alloys and Compounds, 2018, 763: 241−249.

[18] XU Cong, CHENG Hong-wei, LI Guang-shi, LU Chang-yun,

LU Xiong-gang, ZOU Xing-li, XU Qian. Extraction of metals from complex sulfide nickel concentrates by low-temperature chlorination roasting and water leaching [J]. International Journal of Minerals, Metallurgy, and Materials, 2017, 24(4): 377−385.

[19] HUA Zhong-sheng, GENG Ao, TANG Ze-tao, ZHAO Zhuo, LIU Huan, YAO Yong-lin, YANG Yong-xiang. Decomposition behavior and reaction mechanism of $Ce_{0.67}Tb_{0.33}MgAl_{11}O_{19}$ during Na_2CO_3 assisted roasting: Toward efficient recycling of Ce and Tb from waste phosphor [J]. Journal of Environmental Management, 2019, 249: 109383.

[20] ABBASALIZADEH A, SEETHARAMAN S, TENG L D, SRIDHAR S, GRINDER O, IZUMI Y, BARATI M. Highlights of the salt extraction process [J]. JOM, 2013, 65(11): 1552−1558.

[21] HUA Zhong-sheng, WANG Jian, WANG Lei, ZHAO Zhuo, LI Xin-lei, XIAO Yan-ping, YANG Yong-xiang. Selective extraction of rare earth elements from NdFeB scrap by molten chlorides [J]. ACS Sustainable Chemistry & Engineering, 2014, 2(11): 2536−2543.

[22] ZHU Zeng-li, LIU Huan, CHEN Jie-shuang-yang, KONG Hui, XU Liang, HUA Zhong-sheng, ZHAO Zhuo. Electrochemical behavior and electrolytic preparation of lead in eutectic NaCl−KCl melts [J]. Transactions of Nonferrous Metals Society of China, 2020, 30(9): 2568−2576.

[23] LIU Zhao-ting, LU Gui-min, YU Jian-guo. Electrochemical behavior of magnesium ions in chloride melt [J]. Ionics, 2019, 25(6): 2719−2727.

[24] ZHAO Kun, WANG Yao-wu, GAO Feng. Electrochemical extraction of titanium from carbon-doped titanium dioxide precursors by electrolysis in chloride molten salt [J]. Ionics, 2019, 25(12): 6107−6114.

[25] LIU Ya-lan, YUAN Li-yong, LIU Kui, YE Guo-an, ZHANG Mi-lin, HE Hui, TANG Hong-bin, LIN Ru-shan, CHAI Zhi-fang, SHI Wei-qun. Electrochemical extraction of samarium from LiCl−KCl melt by forming Sm−Zn alloys [J]. Electrochimica Acta, 2014, 120: 369−378.

[26] KIM G Y, KIM T J, JANG J, EUN H C, LEE S J. Formation of U–Zn alloys in the molten LiCl−KCl eutectic [J]. Journal of Radioanalytical and Nuclear Chemistry, 2017, 314(1): 529−532.

[27] XUE Yun, ZHOU Zhi-ping, YAN Yong-de, ZHANG Mi-lin, LI Xing, JI De-bin, HAN Wei, ZHANG Meng. Electrochemical co-reduction extraction of neodymium in LiCl−KCl−$ZnCl_2$ molten salt system [J]. Acta Physica Sinica, 2014, 30(9): 1674−1680. (in Chinese)

[28] YASUDA K, SHIMAO T, HAGIWARA R, HOMMA T, NOHIRA T. Electrolytic production of silicon using liquid zinc alloy in molten $CaCl_2$ [J]. Journal of the Electrochemical Society, 2017, 164(8): H5049−H5056.

[29] ZHU Zeng-li, WU Xiao-bin, HUA Zhong-sheng, XU Liang, HE Shi-wei, GENG Ao, YANG Yong-xiang, ZHAO Zhuo. Electrochemical behavior of Dy(III) and formation of Dy−Zn alloy by co-reduction with Zn(II) in eutectic NaCl−KCl melts [J]. Journal of the Electrochemical Society, 2020, 167(12): 122509.

[30] WANG Hong-jun, FENG Ya-li, LI Hao-ran, KANG Jin-xing. Simultaneous extraction of gold and zinc from refractory carbonaceous gold ore by chlorination roasting process [J]. Transactions of Nonferrous Metals Society of China, 2020, 30(4): 1111−1123.

[31] HUA Zhong-sheng, LIU Huan, WANG Jian, HE Ji-wen, XIAO Sai-jun, XIAO Yan-ping, YANG Yong-xiang. Electrochemical behavior of neodymium and formation of Mg−Nd alloys in molten chlorides [J]. ACS Sustainable Chemistry & Engineering, 2017, 5(9): 8089−8096.

[32] HUA Zhong-sheng, WU Xiao-bin, ZHU Zeng-li, HE Ji-wen, HE Shi-wei, LIU Huan, XU Liang, YANG Yong-xiang, ZHAO Zhuo. One-step controllable fabrication of 3D structured self-standing Al_3Ni_2/Ni electrode through molten salt electrolysis for efficient water splitting [J]. Chemical Engineering Journal, 2022, 427: 131743.

[33] ZHANG Zheng, SONG Qiu-shi, JIANG Bao-cheng, XIE Hong-wei, YIN Hua-yi, NING Zhi-qiang, XU Qian. Electrochemically assisted carbonization of Nb in molten salt [J]. Surface and Coatings Technology, 2019, 358: 865−872.

[34] ZHANG H, CHOI S, HAMILTON D E, SIMPSON M F. Electroanalytical measurements of UCl_3 and $CeCl_3$ in molten NaCl−$CaCl_2$ [J]. Journal of the Electrochemical Society, 2021, 168(5): 056521.

[35] CASTRILLEJO Y, BERMEJO M R, AROCAS P D, MARTÍNEZ A M, BARRADO E. Electrochemical behaviour of praseodymium (III) in molten chlorides [J]. Journal of Electroanalytical Chemistry, 2005, 575(1): 61−74.

[36] ZHANG Mi-lin, CHEN Li-jun, HAN Wei, YAN Yong-de, CAO Peng. Electrochemical behavior of Pb(II) in LiCl−KCl−$MgCl_2$−$PbCl_2$ melts on Mo electrode [J]. Transactions of Nonferrous Metals Society of China, 2012, 22(3): 711−716.

[37] BARD A J, FAULKNER L R. Electrochemical methods: Fundamentals and applications [M]. New York: John Wiley & Sons, 2001.

[38] CAI Yan-qing, CHEN Xing-gang, XU Qian, XU Ying. Electrochemical behaviour of tin in a LiCl−KCl eutectic melt [J]. International Journal of Electrochemical Science, 2018, 13: 10786−10797.

[39] LAITY R W, MCINTYRE J D E. Chronopotentiometric diffusion coefficients in fused salts I: Theory [J]. Journal of the American Chemical Society, 1965, 87(17): 3806−3812.

[40] CASSAYRE L, SERP J, SOUCEK P, MALMBECK R, REBIZANT J, GLATZ J P. Electrochemistry of thorium in LiCl−KCl eutectic melts [J]. Electrochimica Acta, 2007, 52(26): 7432−7437.

NaCl−KCl 共熔盐中 Zn^{2+}的电化学还原机理

吴孝彬[1]，朱曾丽[1]，孔 辉[1,2]，樊友奇[1]，程思维[1]，华中胜[1,2]

1. 安徽工业大学 冶金工程学院，马鞍山 243032；
2. 安徽工业大学 冶金工程与资源综合利用安徽省重点实验室，马鞍山 243002

摘 要：为了开发高效、环境友好型冶金粉尘中锌回收技术，提出一种将选择性氯化和熔盐电解相结合的工艺。首先，通过热力学论证上述处理工艺的理论可行性。然后，采用多种暂态电化学测试方法研究 973 K 时 NaCl−KCl 共熔盐中 Zn^{2+}在钨电极上的电化学行为。结果表明，Zn^{2+}的还原过程是一步转移 2 个电子的反应，起始还原电位为−0.74 V (vs Ag/AgCl)；且为受扩散控制的准可逆过程，计算得到 Zn^{2+}的扩散系数为 10^{-5} cm^2/s 数量级。最后，在 NaCl−KCl−$ZnCl_2$ 熔盐中于−1.6 V (vs Ag/AgCl)进行恒电位电解，电解 9.5 h 后获得银白色类球状金属颗粒，经分析证实为金属 Zn。本研究表明，在 NaCl−KCl 共熔盐中直接电解 $ZnCl_2$ 提取金属锌是可行的，为冶金粉尘中锌的高效回收提供了有益的理论参考。

关键词：电化学还原；Zn^{2+}离子；电化学行为；NaCl−KCl 共熔盐；冶金粉尘

(Edited by Wei-ping CHEN)